Article

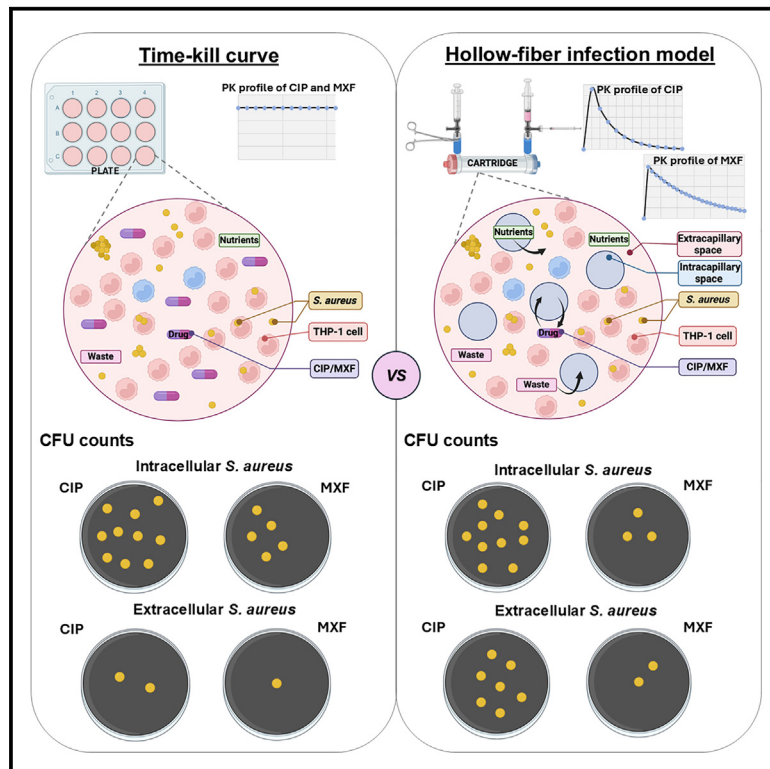# A hollow fiber infection model to study intracellular and extracellular antibiotic activity against *Staphylococcus aureus*

Graphical abstract

Authors

Gwenaëlle Mahieu, Laure Elens, Noémie Prebonnaud, Alexia Chauzy, Françoise Van Bambeke

Correspondence

francoise.vanbambeke@uclouvain.be

In brief

Molecular biology; Neuroscience; Cell

Highlights

- Antibiotic efficacy is influenced by fluctuations in concentrations over time

- Hollow fiber dynamic models (HFIMs) allow to mimic these fluctuations *in vitro*

- HFIM has been adapted here to fluoroquinolones against intracellular *S. aureus*

- Activity differed in dynamic vs static conditions, illustrating the model's relevance

CellPress

Article

A hollow fiber infection model to study intracellular and extracellular antibiotic activity against *Staphylococcus aureus*

Gwenaëlle Mahieu,[1,2] Laure Elens,[2,3] Noémie Prebonnaud,[4,5] Alexia Chauzy,[4] and Françoise Van Bambeke[1,6,*]

[1]Pharmacologie cellulaire et moléculaire, Louvain Drug Research Institute (LDRI), Université catholique de Louvain (UCLouvain), 1200 Brussels, Belgium
[2]Integrated PharmacoMetrics, PharmacoGenomics and Pharmacokinetics (PMGK) Research Group, Louvain Drug Research Institute (LDRI), Université catholique de Louvain (UCLouvain), 1200 Brussels, Belgium
[3]Louvain Centre for Toxicology and Applied Pharmacology (LTAP), Institut de Recherche expérimentale et clinique (IREC), Université catholique de Louvain (UCLouvain), 1200 Brussels, Belgium
[4]Université de Poitiers, INSERM U1070, PHAR2, 86000 Poitiers, France
[5]Laboratoire de Toxicologie-Pharmacocinétique, CHU de Poitiers, Poitiers, France
[6]Lead contact
*Correspondence: francoise.vanbambeke@uclouvain.be
https://doi.org/10.1016/j.isci.2025.112076

SUMMARY

Antibiotic activity against intracellular pathogens is commonly evaluated in static models that do not reproduce plasma concentration fluctuations. However, efficacy is influenced by exposure conditions, related to drug pharmacokinetic profile. This study developed and validated an intracellular pharmacodynamic model using the hollow fiber system, the gold standard for evaluating extracellular antibiotic activity. The activity of fluoroquinolones, i.e., bactericidal antibiotics with intracellular tropism, was studied against intracellular *Staphylococcus aureus*, involved in persistence/recurrence of infections. In this model, moxifloxacin was more effective than in static conditions (0.87 $\log_{10}$ killing gain), while ciprofloxacin kill rate was slower (18 vs. 12 h to achieve 1 $\log_{10}$ killing). These differences were linked to the Cmax/MIC ratio, which was 2.5-fold higher for moxifloxacin but 3.4-fold lower for ciprofloxacin in dynamic vs. static conditions. This model could be applied to other drugs, cell types, or pathogens, offering a tool for optimizing dosing schemes and considering intracellular reservoirs.

INTRODUCTION

Staphylococcus aureus, a Gram-positive bacterium, is a human commensal organism, colonizing 20–30% of individuals on the skin or mucous membrane, such as the nose.[1,2] However, it can also act as an opportunistic pathogen, causing severe infections, including osteomyelitis, pneumonia, or endocarditis that are associated with a risk of mortality.[2,3] Infections caused by *S. aureus* represent a major public health concern, particularly due to the pathogen's ability to develop resistance to antibiotics, as best exemplified by methicillin-resistant *S. aureus* (MRSA).[4,5] On top of that, *S. aureus* is able to invade and persist within mammalian host cells, including phagocytic cells.[2,6,7] These intracellular niches contribute to the persistence and/or recurrence of the infection due to their reduced responsiveness to antibiotics.[7,8] Many previous studies, including some from our laboratory, indicate that this loss of efficacy occurs regardless of their capacity to accumulate within the host cells or colocalize with bacteria in infected subcellular compartments.[9–11] However, all these studies exposed infected cells to constant antibiotic concentrations, which do not mimic the fluctuations of anti-

biotic concentrations over time that bacteria encounter *in vivo*, depending on the drug's pharmacokinetic profile (PK).

Pharmacodynamic (PD) studies clearly demonstrate that the influence of concentration over time is a crucial determinant of antibiotic efficacy, which varies among antibiotic classes. For time-dependent antibiotics, such as β-lactams, efficacy is primarily driven by the duration that bacteria are exposed to concentrations above the minimum inhibitory concentration (MIC). In contrast, concentration-dependent antibiotics, like aminoglycosides, depend on the ratio of the peak concentration (Cmax) to MIC. Many other classes show an intermediate profile, where efficacy is influenced by the global exposure (area under the curve; AUC), with varying impacts of Cmax and exposure time.[12] This is the case for fluoroquinolones, which are considered antibiotics of choice against intracellular bacteria due to their ability to accumulate in both phagocytic and non-phagocytic cells and their proven activity against intracellular bacteria residing in different subcellular compartments (cytosol or vesicles of the phagolysosomal apparatus).[13] To accurately apprehend the impact of concentration vs. time of exposure on their intracellular activity, a model capable of simulating their clinical pharmacokinetic profile is therefore critically needed.
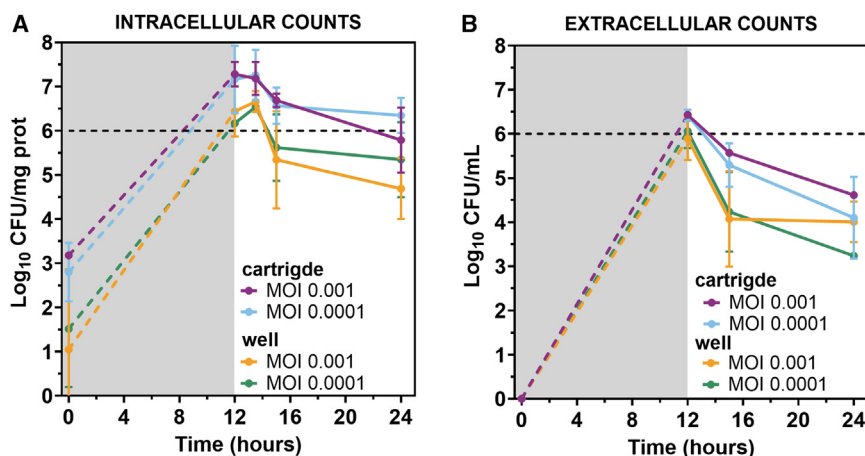
A   INTRACELLULAR COUNTS

B   EXTRACELLULAR COUNTS

Figure 1. Determination of the MOI allowing a 12-h equilibration before reaching the target inoculum of 106 CFU per mg cell protein (intracellular) or per mL (extracellular)

The graphs show the change in the number of colonies forming units (CFU) ($\Delta \log_{10}$ CFU per mg of cell protein in THP-1 monocytes (A) or per mL of culture medium (B) over 24 h of incubation using initial MOI of 0.001 or 0.0001. Dotted line, target inoculum at 12 h, i.e., the end of the equilibration phase that will correspond to time 0 (addition of antibiotics) in further experiments. The gray zone corresponds to this preconditioning phase. Data are means ± SD ($N = 1$, $n = 3$).

The hollow fiber infection model (HFIM) consists of a hollow fiber cartridge supplied with culture fluid that is renewed over time at a predefined rate. To study the efficacy of a given antibiotic under dynamic conditions, the cartridge can be infected, and the fluid supplemented with the antibiotics being studied. The flow rate is then carefully adjusted to simulate the antibiotic pharmacokinetic profile. Samples are collected over time to ensure the simulated profile matches actual drug concentrations and, in parallel, to monitor the number of surviving bacteria. This model is considered the gold standard for studying antibiotic pharmacodynamics *in vitro*.[14] However, to the best of our knowledge, it has only been anecdotally adapted to evaluate antibiotic activity against intracellular bacteria, namely Mycobacteria[15,16] and more recently, *Listeria monocytogenes*.[17] The adaptation is more challenging when dealing with more cytotoxic species like *S. aureus*.

In this work, we successfully established an HFIM of intracellular infection of THP-1 monocytes by a *S. aureus* reference strain. We fully validated the model for bacterial and cell proliferation as well as for cell viability. We then used it to evaluate the activity of two fluoroquinolones, namely ciprofloxacin, a first-generation molecule with modest activity against gram-positive bacteria, and moxifloxacin, one of the most potent and widely used fluoroquinolones against *S. aureus* on the market.[18,19] Finally, we compared the activity observed in the dynamic hollow fiber system with that obtained in a conventional static model of time-kill-curves (TKC), where infected cells are exposed to constant antibiotic concentrations over time.

RESULTS

Minimum inhibitory concentrations

The MIC of ciprofloxacin and moxifloxacin were 0.125 µg mL^{-1} and 0.06 µg mL^{-1}, respectively, before hollow-fiber experiments and remained stable throughout the study.

Setting-up the HFIM experiments

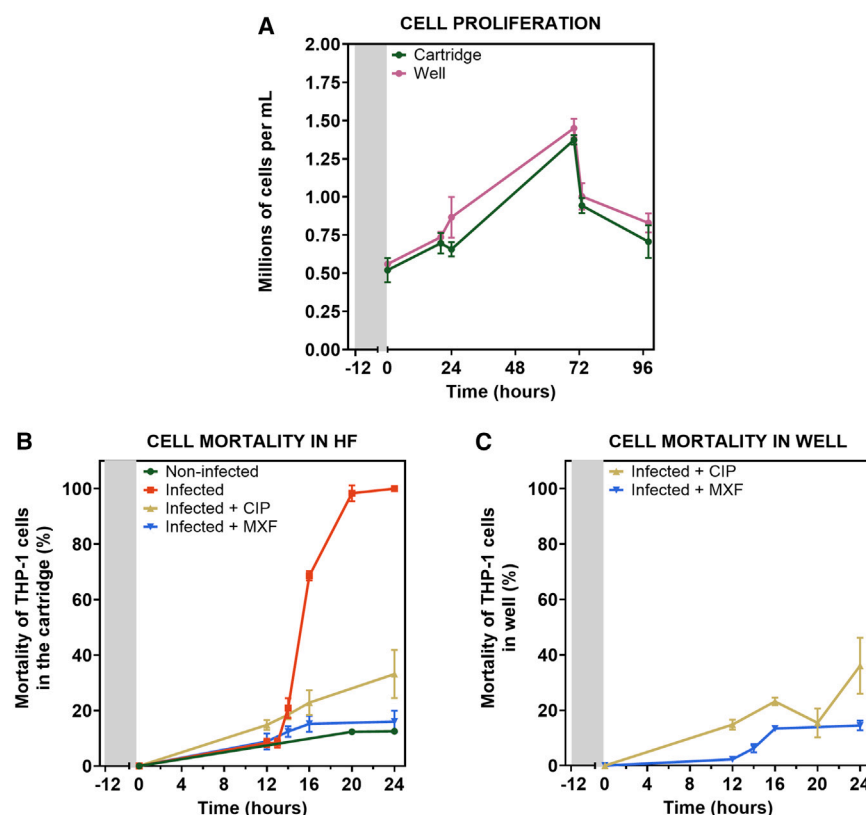Before testing antibiotic activity, we conducted a series of preliminary experiments aiming (1) at evaluating the capacity of the cells to adapt in the HF cartridge and (2) at determining the right Multiplicity of Infection (MOI) to allow at the same time equilibration of the infected cells and adequate infection. Optimization of these conditions was critical for ensuring the validity and reliability of the model.

Determination of the MOI allowing 12-h pre-equilibration of the HF system

Initially, we aimed at determining the optimal MOI that would allow a 12-h equilibration and adaptation period for *S. aureus* infected cells within the cartridge before starting antibiotic treatment.[15] Our goal was to achieve an intracellular inoculum of approximately 10^6 colony-forming unit (CFU) per mg of total cell protein at the end of this preincubation period. This target post-phagocytosis inoculum is typically reached in static experiments using an MOI of 4 bacteria per cell, which is considered adequate for ensuring sufficient detection of surviving bacteria even after exposure to bactericidal antibiotics,[10] while maintaining infected cells viable. To this end, we infected THP-1 cells with two different MOI of *S. aureus* (0.001 and 0.0001) and measured the intracellular and extracellular inoculum after 12 h under two distinct conditions: an "HF condition" where the cells were infected and incubated in the HF cartridge (closed system with no medium renewal) and a "well condition" where the cells were infected and incubated in wells.

Both inocula allowed to reach the desired bacterial load intracellularly (Figure 1A), with the cartridge containing the higher inoculum (MOI = 0.001) showing slightly, but not significantly, higher values compared to the other condition ($\log_{10}$ CFU counts at 12 h: 7.28 ± 0.28 in the cartridge and 6.44 ± 0.57 in the well for MOI = 0.001 [$p \geq 0.05$]; 7.17 ± 0.77 in the cartridge and 6.17 ± 0.04 in the well for MOI = 0.0001 [$p \geq 0.05$]). In the absence of antibiotics, extracellular contamination developed over time, as indicated by the presence of extracellular bacteria in Figure 1B ($\log_{10}$ CFU counts at 12 h: 6.43 ± 0.05 in the cartridge and 5.89 ± 0.49 in the well for MOI = 0.001 [$p \geq 0.05$]; 6.42 ± 0.12 in the cartridge and 6.06 ± 0.38 in the well for MOI = 0.0001 [$p \geq 0.05$]). No significant differences were observed between intracellular and extracellular counts for each inoculum tested.

Figure 2. Cell proliferation and survival in the extracapillary space (ECS) of the HF cartridge vs. in well

(A) proliferation of THP-1 over time, with the number of cells expressed in millions per mL of culture medium.

(B and C) Mortality of THP-1 over time in HF cartridge and well, respectively, expressed as a percentage (%) of dead cells. The gray zone corresponds to the 12 h preconditioning phase. Each data point represents the mean ± SD ($N = 1$, $n = 3$).

1.28 h^{-1} (95% CI, 0.79 to 1.77) and 0.65 h^{-1} (95% CI, 0.42 to 0.89) for ciprofloxacin and moxifloxacin respectively.

Based on these findings, a MOI of 0.0001 was selected for further HFIM and TKC experiments, as this was the lowest inoculum allowing to reach the desired initial infection load with acceptable cell mortality in antibiotic-treated cells during the projected duration of further pharmacological experiments.

Pharmacokinetic profiles in HFIM

PK profiles simulating the IV administration of ciprofloxacin (400 mg twice-daily) and moxifloxacin (400 mg once-daily) were established based on literature data,[20,21] and these simulations aimed at reproducing protein-unbound drug concentrations (Table 1). Experimental concentration-time profiles were then checked in the HF model. The observed and targeted PK parameters, including Cmax, half-life ($T_{1/2}$), time to maximum concentration (Tmax), and AUC, are summarized in Table 2 with PK profiles shown in Figure 3. The observed profiles generally matched the planned values, although for ciprofloxacin, Cmax value were 25% lower and $T_{1/2}$ 28% longer than expected, while for moxifloxacin, Cmax and AUC values were 10% higher and $T_{1/2}$ 10% shorter than expected in the cartridge. These variations are, however, smaller than interindividual variabilities reported in the clinics[22,23] and within the 20% error assumed for simulated data. Moxifloxacin concentrations were also measured intracellularly but close to the limit of quantification (undetectable for ciprofloxacin). The data confirm that moxifloxacin accumulates to high levels in the cells and suggest that higher cellular concentrations are reached in dynamic conditions than in static conditions with, however, a delay of 8 h before reaching the maximum (approx. 100 μg mL^{-1} of cellular volume, considering a cell volume of 5 μL per mg of cell protein).

Cell viability of non-infected vs. infected cells in the HF cartridge vs. well

We then determined whether non-infected and infected THP-1 cells could adapt to a new environment in the cartridge by comparing their viability with that observed in a static well environment (Figure 2). Cell counts and viability were assessed for a MOI of 0.0001 after 12 h of preincubation. When comparing the growth of non-infected cells in both environments, no difference was observed, with a cell count of approximately 1.5 × 10^6 cells mL^{-1} reached after 3 days of culture (panel A) at statistically similar growth rates (k = 0.004571 h^{-1} (cartridge) [95% confidence interval [CI], 0.0002950 to 0.009079] and 0.004356 h^{-1} (well) [95% CI, 0.0005632 to 0.008325]). For longer incubation times, cell numbers started to decline, indicating cell death. Cell mortality was then followed over a 24-h period after the 12 h preconditioning phase, with the same MOI. In the cartridge (panel B), mortality of non-infected cells increased linearly over time, at a rate of 0.55 h^{-1} (95% CI, 0.47 to 0.64). In contrast, infected cells remained viable during 12 h, after which mortality increased rapidly, at a rate of 13.07 h^{-1} (95% CI, 10.54 to 15.61). Importantly, when antibiotics were added to the cartridge at their Cmax, cell viability was maintained over time, yielding mortality rates slightly higher than those observed for non-infected cells (k = 1.39 h^{-1} [95% CI, 1.10 to 1.69] with ciprofloxacin and 0.71 h^{-1} [95% CI, 0.50 to 0.93] with moxifloxacin). Similar experiments conducted in wells (panel C) demonstrated that there was no significant difference in cell mortality between the cartridge and well environments in the presence of antibiotics, with k =

Pharmacodynamic measurements in HFIM and comparison with TKC experiments

The antibacterial activity of ciprofloxacin and moxifloxacin was then examined against *S. aureus* under both dynamic (HFIM) and static conditions (TKC).

In the dynamic HFIM, antibiotic concentrations fluctuate over a 24-h period, simulating *in vivo* pharmacokinetics. In contrast,

Table 1. Moxifloxacin and ciprofloxacin unbound pharmacokinetic parameters simulated in the HFIM

Drug[a]	Cmax (mg mL^{-1})	Tinf (hours)	τ (hours)	$T_{1/2}$ (hours)	Cl (mL min^{-1})	Reference
Moxifloxacin	2.41	1	24	8.49	0.49	Stass, and Kubitza[21]
Ciprofloxacin	2.80	1	12	1.80	2.31	Lettieri et al.[20]

Cmax, maximum serum concentration; Tinf, infusion duration; τ, dosing interval; $T_{1/2}$, elimination half-life; Cl, clearance.
[a]Simulated with the HF-app: https://varacli.shinyapps.io/hollow_fiber_app/.

the static TKC model uses fixed antibiotic concentrations over a 24-h period. Here, we selected a concentration equivalent (a) to human free Cmax that simulates the highest concentration to which bacteria could be exposed extracellularly but overestimating the 24-h exposure, or (b) to free AUC that mimics adequately the global exposure over time but not the peak effect considered as important for fluoroquinolones. In both models, antibacterial activity was assessed separately for intracellular bacteria infecting THP-1 and for extracellular bacteria escaping from cells in the culture medium.

In the absence of antibiotics, intracellular bacteria proliferated significantly in both models (Figure 4). Intracellular bacteria gained 1.1–1.3 $\log_{10}$ CFU per mg of total cell proteins after 5 h in both models, and approximately 2–3 $\log_{10}$ CFU per mg of total cell proteins in the HFIM (panels A, B) or the TKC model (panels C, D), respectively, over the 24-h period.

Both antibiotics could reduce bacterial counts of extracellular and intracellular bacteria, with an initial rapid killing phase followed by a plateau. In both the dynamic and static models, the two antibiotics were more active against extracellular than intracellular bacteria, and moxifloxacin achieved faster and more pronounced reduction in bacterial counts compared to ciprofloxacin. Table 3 provides a detailed comparison of the pharmacodynamic parameters characterizing their activities. We calculated minimal durations for killing (MDK) for different reductions in inoculum, a parameter usually used to characterize antibiotic tolerance[24] but also adequate to compare kill rates, especially when showing a biphasic profile, as observed here. This biphasic killing, already observed in previous reports, has been attributed

to the presence of a tolerant subpopulation of bacteria, described as persisters.[11,24] We also estimated Emax, i.e., the maximal killing effect, corresponding to the plateau value of the exponential decay equation fitted to the data.

In the context of the present study, the comparison of each drug in the dynamic (HFIM) and the static (TKC) models is particularly important (see also Figure S2).

Ciprofloxacin was equally effective (similar Emax) against intracellular bacteria in the HFIM and TKC model exposed to human free Cmax during 24 h. However, it was less effective in static conditions simulating the human free AUC$_{24h}$ (Figures 4A and 4C; Figure S2C). Furthermore, ciprofloxacin exhibited slower bacterial killing (longer MDK$_{90}$) in the HFIM than in static conditions (Table 3). Extracellularly, ciprofloxacin demonstrated faster (shorter MDK$_{90}$) and more pronounced (more negative Emax) killing at free human Cmax in TKC than in the HFIM or in static conditions mimicking AUC (Table 3; Figures 4A and 4C; Figure S2E). The two latter conditions of exposure achieved a similar Emax, although faster killing was observed in the HFIM (Table 3).

Moxifloxacin caused significantly more pronounced killing intracellularly in the dynamic model than in static conditions, but MDK$_{90}$ or MDK$_{99}$ (when it was achieved) values were short and similar in both types of models (Figures 4B and 4D; Figure S2D; Table 3). Extracellularly, killing was slightly more pronounced (more negative Emax, limit of significance based on overlap of Cl) and rapid (shorter MDK values) in static conditions compared to dynamic conditions (Table 3; Figures 4B and 4D; Figure S2F).

Table 2. Target and measured pharmacokinetic parameters in the HFIM experiment

Parameters[a]		Ciprofloxacin (CIP)		Moxifloxacin (MXF)	
		Target[b]	Actual	Target[b]	Actual
Cmax (μg mL^{-1})	Central	2.80	2.69 ± 0.12	2.41	2.25 ± 0.20
	Cartridge	2.80	2.12 ± 0.091	2.41	2.67 ± 0.15
$T_{1/2}$ (h)	Central	1.80	1.45 ± 0.81	8.49	7.95 ± 3.37
	Cartridge	1.80	2.31 ± 1.46	8.49	7.80 ± 2.04
T_{max} (h)	Central	1.00	1.00	1.00	1.00
	Cartridge	1.00	1.00	1.00	1.00
Auc$_{0-24}$ (mg.h L^{-1})	Central	17.31	17.21 ± 0.25	26.41	24.79 ± 1.75
	Cartridge	17.31	18.00 ± 0.70	26.41	28.50 ± 1.42
AUC$_{0-24}$/MIC	Cartridge	138.48	144 ± 5.6	440.17	475 ± 29.17
Cmax/MIC	Cartridge	22.24	16.96 ± 0.73	39.83	44.5 ± 2.5

[a]Cmax, maximum serum concentration; $T_{1/2}$, elimination half-life; T_{max}, time at which Cmax is reached; AUC$_{0-24}$, area under the 24-h concentration-time curve. All observed results are mean of 3 independent experiments (N = 3) ± SEM.
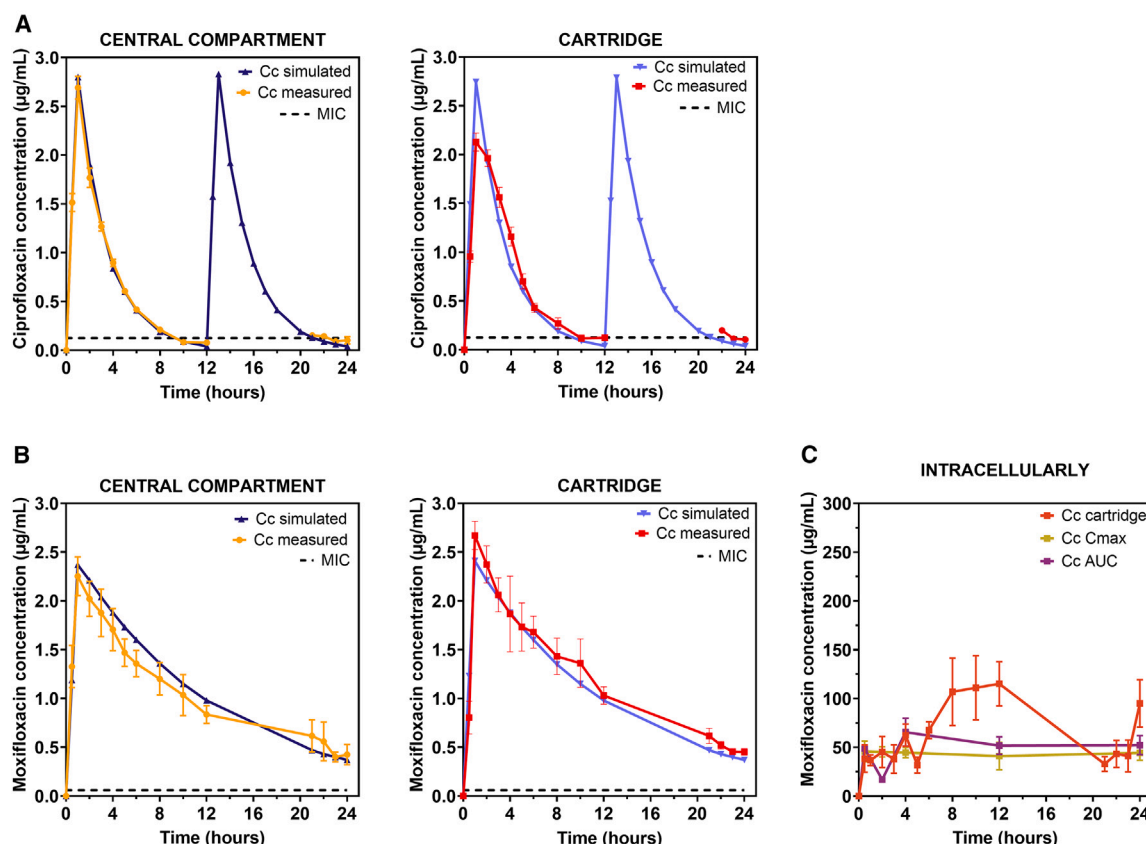[b]An error margin of ±20% is assumed for these values.

Figure 3. Fluoroquinolone concentration-time profile (PK) in the hollow fiber system model and intracellularly

(A) PK profile of ciprofloxacin for 400 mg twice daily dosing schedule by IV route.

(B) PK profile of moxifloxacin for 400 mg once-daily dosing schedule by IV route. Data are shown for the fluids sampled in the central compartment and in the cartridge, respectively. Simulated values were obtained with the HF-App. Measured values are shown as means ± SEM of three independent replicates (when non visible, error bars are smaller than the symbol size). Dashed line, MIC of the antibiotic against the studied strain.

(C) Moxifloxacin concentration measured inside the THP-1 cells, either for cells collected from the cartridge or from wells exposed to concentrations mimicking free Cmax or AUC. Cellular concentrations are expressed in $\mu g\ mL^{-1}$ of cell volume, considering a cell volume of 5 μL per mg cell protein.[10] Limit of quantification in fluids or cell lysates (LOQ) for CIP = 0.040 $\mu g\ mL^{-1}$ (not detected in cell lysates) and LOQ for MXF = 0.015 $\mu g\ mL^{-1}$.

DISCUSSION

Due to the challenge of treating *S. aureus* intracellular infections with current antibiotics, there is an urgent need to optimize their use to ensure bacterial killing and the prevention of resistance. In this study, we successfully developed a dynamic *S. aureus* intracellular infection model, representing a significant advancement in simulating the interaction between antibiotics and bacteria within host cells.

While similar approaches have previously been applied to other intracellular pathogens such as *Listeria monocytogenes*[17] and *Mycobacterium* spp.,[15,16] adapting the HFIM to intracellular *S. aureus* presented a unique challenge, particularly due to its ability to escape from the host cells by killing them in order to disseminate in the tissues.[25] To our knowledge, this is the first study using the HFIM model to assess the activity of antibiotics over 24 h on both intracellular and extracellular *S. aureus*.

Previous HFIM studies evaluating antimicrobial activity against extracellular *S. aureus* have primarily focused on MRSA and bio-

film-related infections. Some of these studies assessed the efficacy of specific antimicrobial agents in reducing MRSA virulence.[26] Others compared antibiotic combinations against biofilm and planktonic bacteria.[27] Additionally, other works have examined moxifloxacin[28] and ciprofloxacin[29] efficacy against extracellular, and not intracellular, *S. aureus* in the HFIM, but they did not consider the unbound fraction of the antibiotics, which is required to accurately assess drug activity.

In the present study, key parameters were optimized in order to adapt the model to intracellular *S. aureus*. These include the inoculum size, taking into account the need of an equilibrium time in the cartridge, and the proliferation and viability of THP-1 cells within the cartridge. These optimizations, not described in the previously published models of intracellular HFIM, ensured that antibiotic effects were accurately measured without interference from confounding factors such as the stress caused by the infection process or the system itself. The 12-h equilibrium period was specifically used to promote the proliferation of the intracellular inoculum, achieving a bacterial density
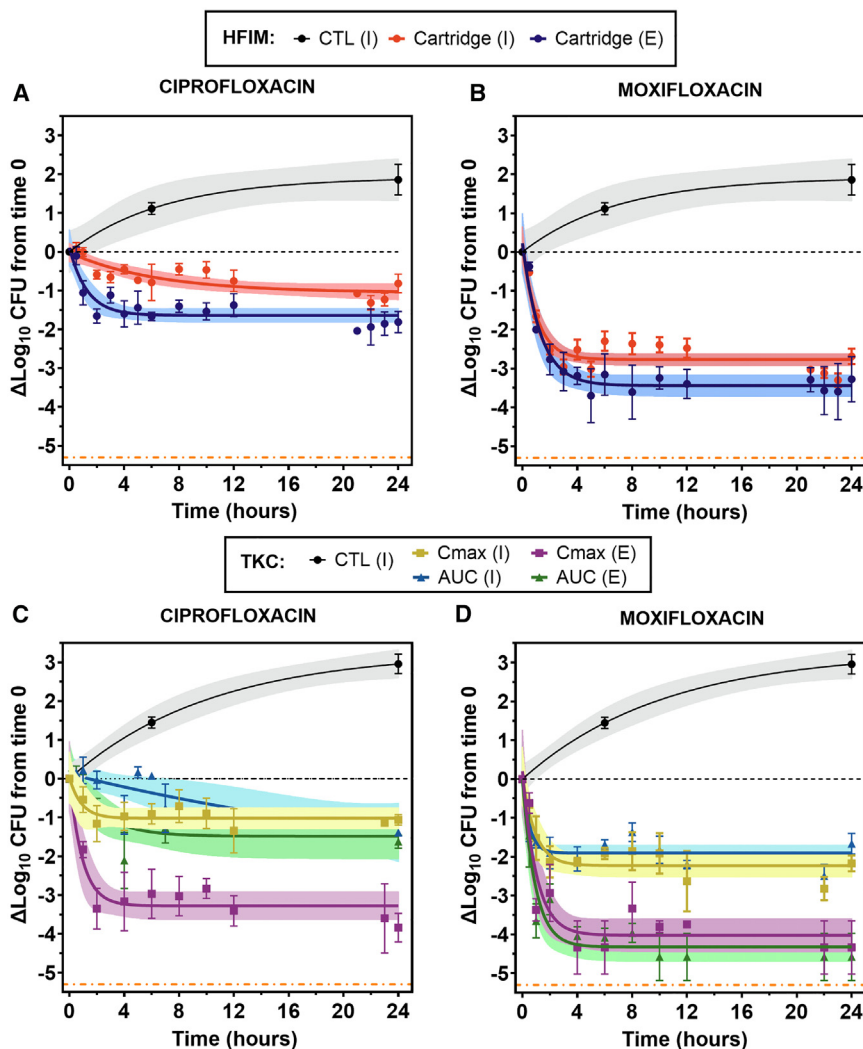
Figure 4. Fluoroquinolone activities in dynamic (HFIM) and static (TKC) conditions against extracellular and intracellular forms S. aureus

The graphs show the change in the number of colonies forming units (CFU) ($\Delta \log_{10}$ CFU) per mL of culture medium (extracellular fraction; [E]) or in THP-1 monocytes (intracellular; [I]) per mg of cell protein over the time of incubation as compared to the initial inoculum. HFIM: ciprofloxacin (A) and moxifloxacin (B) concentrations fluctuate over time in the cartridge to mimic human PK profiles for unbound drugs (see Figure 3). TKC: ciprofloxacin (C) and moxifloxacin (D) were added at their maximal serum concentration (Cmax, free drug: 2.8 µg mL^{-1} for ciprofloxacin and 2.4 µg mL^{-1} for moxifloxacin) or at 0.7 µg mL^{-1} for ciprofloxacin and 1.1 µg mL^{-1} for moxifloxacin to simulate the free 24 h area under the concentration-time (AUC) reached in humans. Black dotted line: apparent static effect. Orange dotted line: theoretical limit of detection (1 CFU/plate). Data are means ± SEM with 95% CI; N = 2–3, n = 1. See also Figure S2.

negative bacteria such as *Escherichia coli*.[32] In contrast, moxifloxacin demonstrates strong intracellular activity against *S. aureus*, though complete eradication was not observed, consistent with existing literature.[10,11]

Notably, moxifloxacin demonstrated higher intracellular efficacy in the dynamic HFIM system as compared to traditional TKC experiments. Comparing these two systems (see Figure S2 for a direct comparison of different experimental conditions for each drug) is novel for intracellular bacteria, as previous studies with *L. monocytogenes*[17] or *Mycobacteria* spp.[15,16] did not performed

of approximately 6 $\log_{10}$ CFU after 12 h, previously defined as adequate for assessing antibiotic activity.[10,30,31] During this period, some intracellular bacteria were released from THP-1 cells due to natural cell death, forming an extracellular population that was also exposed to fluctuating drug concentrations, further enhancing the physiological relevance of the model. When antibiotics were introduced, this contamination was modest, and the intracellular inoculum was well controlled, allowing experiments to be conducted for up to 24 h while maintaining acceptable levels of cell mortality. Moreover, we showed that non-infected THP-1 cells survived and proliferated at rates comparable to standard conditions (in wells), confirming that the system environment does not negatively affect cellular health. These results validate the robustness and physiological relevance of our model for studying intracellular and extracellular forms of *S. aureus*.

In this optimized model, our findings highlight the limited activity of ciprofloxacin against intracellular *S. aureus*, which aligns with its established efficacy profile, primarily targeting gram-

TKC experiments in parallel. The differences observed between HFIM and TKC may be attributed to variations in the experimental setup. We observed higher accumulation of moxifloxacin inside THP-1 cells in the HFIM, potentially due to improved medium renewal in the dynamic system. This medium refreshment could reduce the accumulation of toxic cell debris and ensure sustained nutrient availability, supporting cell viability better than a well environment. Conversely, the intracellular activity of ciprofloxacin in the HFIM was lower (vs. TKC at Cmax) or similar (vs. TKC simulating AUC) as compared to static models. We were unable to detect ciprofloxacin intracellularly in the HFIM to confirm this difference, but previous experiments in static models indicate that ciprofloxacin accumulates at lower levels and at a slower rate than moxifloxacin.[33] A delay in accumulation is observed for moxifloxacin in the HFIM despite its almost instantaneous accumulation in static conditions.[34] We may therefore suspect a similar delay occurs for the less diffusible ciprofloxacin, explaining its slower killing in the HFIM.

Table 3. Comparison of minimal duration of killing (MDK) and maximal efficacy (Emax) values of fluoroquinolones against extracellular and intracellular *S. aureus,* under dynamic (HF) and static (TKC) conditions

Conditions[a,b]	Applied treatment	MDK$_{90}$ (1 Log)	MDK$_{99}$ (2 Log)	MDK$_{99.9}$ (3 Log)	MDK$_{99.99}$ (4 Log)	Emax
Dynamic (Intra)	CIP	18 h	N/A[c]	N/A	N/A	−1.05 log$_{10}$ [95% CI, −1.33 to −0.77]
	MXF	0.5 h	1.5 h	N/A	N/A	−2.77 log$_{10}$ [95% CI, −2.93 to −2.61]
Dynamic (Extra)	CIP	1.5 h	N/A	N/A	N/A	−1.64 log$_{10}$ [95% CI, −1.83 to −1.45]
	MXF	0.5 h	1 h	3 h	N/A	−3.44 log$_{10}$ [95% CI, −3.72 to −3.16]
Static (Intra)	CIP Cmax	3 h	N/A	N/A	N/A	−1.02 log$_{10}$ [95% CI, −1.30 to −0.74]
	CIP AUC	12 h	N/A	N/A	N/A	N/A[d]
	MXF Cmax	0.75 h	2 h	N/A	N/A	−2.23 log$_{10}$ [95% CI, −2.53 to −1.93]
	MXF AUC	0.5 h	N/A	N/A	N/A	−1.90 log$_{10}$ [95% CI, −2.12 to −1.69]
Static (Extra)	CIP Cmax	0.5 h	1 h	2.5 h	N/A	−3.28 log$_{10}$ [95% CI, −3.65 to −2.91]
	CIP AUC	2.5 h	N/A	N/A	N/A	−1.44 log$_{10}$ [95% CI, −2.09 to 0.87]
	MXF Cmax	0.5 h	0.75 h	1.5 h	6 h	−4.02 log$_{10}$ [95% CI, −4.45 to −3.59]
	MXF AUC	0.25 h	0.5 h	1 h	2.5 h	−4.32 log$_{10}$ [95% CI, −4.70 to −3.94]

[a]Estimated as the time needed to achieve 90% (1 log$_{10}$), 99% (2 log$_{10}$), 99.9% (3 log$_{10}$), or 99.99% (4 log$_{10}$) killing based on the equation of the exponential decay curve describing activity over time.

[b]Value of the plateau in the equation of the exponential decay curve describing activity over time. These values are expressed as log$_{10}$ reduction from the initial (i.e., before the drug addition) inoculum (values in log$_{10}$ CFU per mg cell protein (intra) or mL (extra) for control of ciprofloxacin and moxifloxacin experiments [mean ± SD] are respectively: Dynamic, intra: 6.98 ± 0.35 and 6.93 ± 0.07; Dynamic, extra: 5.63 ± 0.47 and 5.21 ± 0.61; Static, intra: 6.24 ± 0.49 and 5.59 ± 0.22; Static, extra: 5.26 ± 0.59 and 4.33 ± 1.18).

[c]N/A, Not Achieved.

[d]Plateau value not reached in this condition.

Regarding extracellular activity, both fluoroquinolones exhibited high efficacy, which can be attributed to their favorable PK/PD parameters. Notably, the AUC$_{0-24h}$/MIC ratio was well above 125 and the Cmax/MIC ratio was also above 10 for both antibiotics in the HFIM. These threshold values are correlated with positive clinical and microbiological outcomes *in vivo* and in the clinics.[18,35] Moreover, the higher AUC$_{0-24h}$/MIC ratio (475 vs. 144 h^{-1}) and Cmax/MIC ratio (44 vs. 17) justifies the faster and better response observed with moxifloxacin compared to ciprofloxacin. In static conditions at Cmax, the AUC$_{0-24h}$/MIC ratio for both drugs is even higher, which explains the better efficacy observed, especially for ciprofloxacin in these conditions (AUC$_{0-24h}$/MIC ratios of 960 and 538 h^{-1} for moxifloxacin and ciprofloxacin, respectively; i.e., values 2 to 3-fold higher than in dynamic conditions). Since fluoroquinolones are Cmax/MIC and AUC$_{0-24h}$/MIC-dependent antibiotics, we also evaluated their activity in static conditions mimicking AUC$_{0-24h}$. In these conditions, the Cmax/MIC ratio decreased from 40 to 18.33 for moxifloxacin and from 22.4 to 5.6 for ciprofloxacin. This reduction does not affect the activity of moxifloxacin but diminishes ciprofloxacin's efficacy (Figure S2), as it no longer meets the required threshold value of 10 for the Cmax/MIC parameter, predictive of high efficacy.[18,35]

Conclusion

In conclusion, the HFIM adapted to intracellular infection by *S. aureus* developed in this study provides a valuable tool for optimizing treatment strategies with conventional drugs and evaluating the efficacy of new compounds in targeting *S. aureus* intracellular infections. Although it does not fully replicate all aspects of the clinics, this model offers several advantages. First, it could be extended to other drugs or other strains, or adapted for specific purposes such as the detection of rare resistant mutants, which is sometimes challenging or nonfeasible with *in vivo* models for ethical reasons.[36] Second, it allows for repetitive sampling, like blood sampling in patients, facilitating the monitoring of drug PK and of the infection dynamics over time. Lastly, the system accurately mimics the PK profiles observed in patients, making it a robust and reliable tool to establish optimized dosing regimens of already available or newly developed drugs, considering the intracellular component of the infection.

Limitations of the study

Despite its novelty, this study has some limitations. First, THP-1 cells, a permissive monocytic cell line, do not fully mimic the diversity and functionality of primary immune cells.[37] Further

adaptation of the model could incorporate peripheral blood mononuclear cells (PBMCs), or other cell types, including bronchial epithelial cells, keratinocytes, or osteoblasts where *S. aureus* is also known to survive,[38] However, this represents an even more complex challenge, as adherent cells may clog the pores of the fibers. Second, the experiments were conducted in a simplified *in vitro* environment, lacking a complete immune response involving other cell types and immune defense mechanisms. Third, the short duration of the experiments, limited to 24 h, restricts the ability to observe the global effect of a full course treatment of 5–14 days[39] Fourth, highly sensitive methods are needed to quantify intracellular antibiotics, as only small volume aliquots can be taken out of the system to maintain its equilibrium. Lastly, a single reference strain has been used to develop the model. A similar set-up can be used to adapt it to relevant clinical isolates, starting by those already used in the past to successfully infect THP-1 cells.[40]

Nevertheless, by simulating *in vivo* exposure, the HFIM may also help to better mimic human PK profiles, especially the free drug concentrations, than animal models. Protein binding is indeed variable among species, as exemplified by the lower protein binding of ciprofloxacin (10%) in mice.[41] Finally, another advantage is that the dynamic conditions of this newly developed intracellular HFIM may provide data of better predictive value compared to static assays (TKC). In particular, we noticed significant differences in efficacy or kill rates between the two models.

RESOURCE AVAILABILITY

Lead contact
Further information and requests for resources should be directed to and will be fulfilled by the lead contact Françoise Van Bambeke (francoise.vanbambeke@uclouvain.be).

Materials availability
This study did not generate new unique reagents.

Data and code availability
- Data: All datasets generated during this study are available upon request from the lead contact.
- Code: No code was generated in this study.
- Misc.: No additional unique resource was used in this study.

AUTHOR CONTRIBUTIONS

G.M, F.V.B., and L.E. designed the research; G.M. conducted the experiments; A.C. an N.P. shared their expertise in HFIM models; G.M. and F.V.B. wrote the manuscript; all authors reviewed and approved the final version of the document.

DECLARATION OF INTERESTS

The authors declare no conflict of interest.

DECLARATION OF GENERATIVE AI AND AI-ASSISTED TECHNOLOGIES

During the preparation of this manuscript, the authors utilized Co-PILOT to improve the readability and language of the manuscript. Following the use of these tools, the entire manuscript was thoroughly reviewed and edited by the authors.

STAR★METHODS

Detailed methods are provided in the online version of this paper and include the following:

- KEY RESOURCES TABLE
- EXPERIMENTAL MODEL AND STUDY PARTICIPANT DETAILS
  - Drugs and chemicals
  - Bacterial strain and cells
- METHOD DETAILS
  - Intracellular infection
  - Hollow fiber infection model (HFIM)
  - Materials
  - Set-up
  - Simulation of PK profiles in the HFIM
  - Pharmacokinetic (PK) measurements in HFIM
  - Both drugs ware assayed by HPLC-MS/MS
  - Pharmacodynamic (PD) measurements in HFIM
  - Time kill-curves (TKC)
  - Cell viability
- QUANTIFICATION AND STATISTICAL ANALYSIS

SUPPLEMENTAL INFORMATION

Supplemental information can be found online at https://doi.org/10.1016/j.isci.2025.112076.

REFERENCES

1. Williams, R.E. (1963). Healthy carriage of Staphylococcus aureus: Its prevalence and importance. Bacteriol. Rev. *27*, 56–71. https://doi.org/10.1128/br.27.1.56-71.1963.

2. Goormaghtigh, F., and Van Bambeke, F. (2024). Understanding Staphylococcus aureus internalisation and induction of antimicrobial tolerance. Expert Rev. Anti Infect. Ther. *22*, 87–101. https://doi.org/10.1080/14787210.2024.2303018.

3. Lowy, F.D. (1998). *Staphylococcus aureus* Infections. N. Engl. J. Med. *339*, 520–532. https://doi.org/10.1056/NEJM199808203390806.

4. (2024). WHO Bacterial Priority Pathogens List 2024 Bacterial Pathogens of Public Health Importance, to Guide Research, Development, and Strategies to Prevent and Control Antimicrobial Resistance (World Health Organization). https://www.who.int/publications/i/item/9789240093461.

5. Turner, N.A., Sharma-Kuinkel, B.K., Maskarinec, S.A., Eichenberger, E.M., Shah, P.P., Carugati, M., Holland, T.L., and Fowler, V.G. (2019). Methicillin-resistant Staphylococcus aureus: An overview of basic and clinical research. Nat. Rev. Microbiol. *17*, 203–218. https://doi.org/10.1038/s41579-018-0147-4.

6. Hébert, A., Sayasith, K., Sénéchal, S., Dubreuil, P., and Lagacé, J. (2000). Demonstration of intracellular *Staphylococcus aureus* in bovine mastitis

alveolar cells and macrophages isolated from naturally infected cow milk. FEMS Microbiol. Lett. *193*, 57–62. https://doi.org/10.1111/j.1574-6968.2000.tb09402.x.

7. Garzoni, C., and Kelley, W.L. (2009). Staphylococcus aureus: New evidence for intracellular persistence. Trends Microbiol. *17*, 59–65. https://doi.org/10.1016/j.tim.2008.11.005.

8. Volk, C.F., Proctor, R.A., and Rose, W.E. (2024). The Complex Intracellular Lifecycle of Staphylococcus aureus Contributes to Reduced Antibiotic Efficacy and Persistent Bacteremia. Int. J. Mol. Sci. *25*, 6486. https://doi.org/10.3390/ijms25126486.

9. Vallet, C.M., Marquez, B., Ngabirano, E., Lemaire, S., Mingeot-Leclercq, M.-P., Tulkens, P.M., and Van Bambeke, F. (2011). Cellular accumulation of fluoroquinolones is not predictive of their intracellular activity: Studies with gemifloxacin, moxifloxacin and ciprofloxacin in a pharmacokinetic/pharmacodynamic model of uninfected and infected macrophages. Int. J. Antimicrob. Agents *38*, 249–256. https://doi.org/10.1016/j.ijantimicag.2011.05.011.

10. Barcia-Macay, M., Seral, C., Mingeot-Leclercq, M.-P., Tulkens, P.M., and Van Bambeke, F. (2006). Pharmacodynamic Evaluation of the Intracellular Activities of Antibiotics against *Staphylococcus aureus* in a Model of THP-1 Macrophages. Antimicrob. Agents Chemother. *50*, 841–851. https://doi.org/10.1128/AAC.50.3.841-851.2006.

11. Peyrusson, F., Varet, H., Nguyen, T.K., Legendre, R., Sismeiro, O., Coppée, J.-Y., Wolz, C., Tenson, T., and Van Bambeke, F. (2020). Intracellular Staphylococcus aureus persisters upon antibiotic exposure. Nat. Commun. *11*, 2200. https://doi.org/10.1038/s41467-020-15966-7.

12. Craig, W.A. (2001). Does the dose matter? Clin. Infect. Dis. *33*, S233–S237. https://doi.org/10.1086/321854.

13. Van Bambeke, F., Barcia-Macay, M., Lemaire, S., and Tulkens, P.M. (2006). Cellular pharmacodynamics and pharmacokinetics of antibiotics: Current views and perspectives. Curr. Opin. Drug Discov. Dev *9*, 218–230. https://www.facm.ucl.ac.be/Full-texts-FACM/Vanbambeke-2006-1.pdf.

14. Cadwell, J.J.S. (2012). The Hollow Fiber Infection Model for Antimicrobial Pharmacodynamics and Pharmacokinetics. Adv. Pharmacoepidemiol. Drug Saf. *S01*. https://doi.org/10.4172/2167-1052.s1-007.

15. Ruth, M.M., Raaijmakers, J., Van Den Hombergh, E., Aarnoutse, R., Svensson, E.M., Susanto, B.O., Simonsson, U.S.H., Wertheim, H., Hoefsloot, W., and Van Ingen, J. (2022). Standard therapy of Mycobacterium avium complex pulmonary disease shows limited efficacy in an open source hollow fibre system that simulates human plasma and epithelial lining fluid pharmacokinetics. Clin. Microbiol. Infect. *28*, 448.e1. https://doi.org/10.1016/j.cmi.2021.07.015.

16. Srivastava, S., Pasipanodya, J., Sherman, C.M., Meek, C., Leff, R., and Gumbo, T. (2015). Rapid Drug Tolerance and Dramatic Sterilizing Effect of Moxifloxacin Monotherapy in a Novel Hollow-Fiber Model of Intracellular Mycobacterium kansasii Disease. Antimicrob. Agents Chemother. *59*, 2273–2279. https://doi.org/10.1128/AAC.04441-14.

17. Patel, S., Chapagain, M., Mason, C., Gingrich, M., Athale, S., Ribble, W., Hoang, T., Day, J., Sun, X., Jarvis, T., et al. (2022). Potency of the novel PolC DNA polymerase inhibitor CRS0540 in a disseminated *Listeria monocytogenes* intracellular hollow-fibre model. J. Antimicrob. Chemother. *77*, 2876–2885. https://doi.org/10.1093/jac/dkac269.

18. Van Bambeke, F., Michot, J.-M., Van Eldere, J., and Tulkens, P.M. (2005). Quinolones in 2005: An update. Clin. Microbiol. Infect. *11*, 256–280. https://doi.org/10.1111/j.1469-0691.2005.01131.x.

19. The European Committee on Antimicrobial Susceptibility Testing (EUCAST). MIC ditributions. Retrieved January 22, 2025, from https://mic.eucast.org/

20. Lettieri, J.T., Rogge, M.C., Kaiser, L., Echols, R.M., and Heller, A.H. (1992). Pharmacokinetic profiles of ciprofloxacin after single intravenous and oral doses. Antimicrob. Agents Chemother. *36*, 993–996. https://doi.org/10.1128/AAC.36.5.993.

21. Stass, H., and Kubitza, D. (1999). Pharmacokinetics and elimination of moxifloxacin after oral and intravenous administration in man. J. Antimicrob. Chemother. *43*, 83–90. https://doi.org/10.1093/jac/43.suppl_2.83.

22. Szałek, E., Tomczak, H., Kamińska, A., Grabowski, T., Smuszkiewicz, P., Matysiak, K., Wolc, A., Kaczmarek, Z., and Grześkowiak, E. (2012). Pharmacokinetics and pharmacodynamics of ciprofloxacin in critically ill patients after the first intravenous administration of 400 mg. Adv. Med. Sci. *57*, 217–223. https://doi.org/10.2478/v10039-012-0028-4.

23. Chatzika, K., Manika, K., Kontou, P., Pitsiou, G., Papakosta, D., Zarogoulidis, K., and Kioumis, I. (2014). Moxifloxacin Pharmacokinetics and Pleural Fluid Penetration in Patients with Pleural Effusion. Antimicrob. Agents Chemother. *58*, 1315–1319. https://doi.org/10.1128/AAC.02291-13.

24. Balaban, N.Q., Helaine, S., Lewis, K., Ackermann, M., Aldridge, B., Andersson, D.I., Brynildsen, M.P., Bumann, D., Camilli, A., Collins, J.J., et al. (2019). Definitions and guidelines for research on antibiotic persistence. Nat. Rev. Microbiol. *17*, 441–448. https://doi.org/10.1038/s41579-019-0196-3.

25. Flannagan, R.S., Heit, B., and Heinrichs, D.E. (2016). Intracellular replication of *Staphylococcus aureus* in mature phagolysosomes in macrophages precedes host cell death, and bacterial escape and dissemination: S. aureus replicates in mature phagolysosomes in macrophages. Cell. Microbiol. *18*, 514–535. https://doi.org/10.1111/cmi.12527.

26. Shukla, S.K., Carter, T.C., Ye, Z., Pantrangi, M., and Rose, W.E. (2020). Modeling of Effective Antimicrobials to Reduce Staphylococcus aureus Virulence Gene Expression Using a Two-Compartment Hollow Fiber Infection Model. Toxins *12*, 69. https://doi.org/10.3390/toxins12020069.

27. Broussou, D.C., Lacroix, M.Z., Toutain, P.-L., Woehrlé, F., El Garch, F., Bousquet-Melou, A., and Ferran, A.A. (2018). Differential Activity of the Combination of Vancomycin and Amikacin on Planktonic vs. Biofilm-Growing Staphylococcus aureus Bacteria in a Hollow Fiber Infection Model. Front. Microbiol. *9*, 572. https://doi.org/10.3389/fmicb.2018.00572.

28. Lister, P.D. (2001). Pharmacodynamics of Moxifloxacin and Levofloxacin against Staphylococcus aureus and Staphylococcus epidermidis in an In Vitro Pharmacodynamic Model. Clin. Infect. Dis. *32*, S33–S38. https://doi.org/10.1086/319374.

29. Marchbanks, C.R., McKiel, J.R., Gilbert, D.H., Robillard, N.J., Painter, B., Zinner, S.H., and Dudley, M.N. (1993). Dose ranging and fractionation of intravenous ciprofloxacin against Pseudomonas aeruginosa and Staphylococcus aureus in an in vitro model of infection. Antimicrob. Agents Chemother. *37*, 1756–1763. https://doi.org/10.1128/AAC.37.9.1756.

30. Lemaire, S., Van Bambeke, F., Mingeot-Leclercq, M.-P., and Tulkens, P.M. (2005). Activity of three β-lactams (ertapenem, meropenem and ampicillin) against intraphagocytic Listeria monocytogenes and Staphylococcus aureus. J. Antimicrob. Chemother. *55*, 897–904. https://doi.org/10.1093/jac/dki094.

31. Brinch, K.S., Sandberg, A., Baudoux, P., Van Bambeke, F., Tulkens, P.M., Frimodt-Møller, N., Høiby, N., and Kristensen, H.-H. (2009). Plectasin Shows Intracellular Activity against *Staphylococcus aureus* in Human THP-1 Monocytes and in a Mouse Peritonitis Model. Antimicrob. Agents Chemother. *53*, 4801–4808. https://doi.org/10.1128/AAC.00685-09.

32. Kerkez, I., Tulkens, P.M., Tenson, T., Van Bambeke, F., and Putriņš, M. (2021). Uropathogenic Escherichia coli Shows Antibiotic Tolerance and Growth Heterogeneity in an *In Vitro* Model of Intracellular Infection. Antimicrob. Agents Chemother. *65*, e01468. https://doi.org/10.1128/AAC.01468-21.

33. Michot, J.-M., Van Bambeke, F., Mingeot-Leclercq, M.-P., and Tulkens, P.M. (2004). Active efflux of ciprofloxacin from J774 macrophages through an MRP-like transporter. Antimicrob. Agents Chemother. *48*, 2673–2682. https://doi.org/10.1128/AAC.48.7.2673-2682.2004.

34. Michot, J.-M., Seral, C., Van Bambeke, F., Mingeot-Leclercq, M.-P., and Tulkens, P.M. (2005). Influence of efflux transporters on the accumulation and efflux of four quinolones (ciprofloxacin, levofloxacin, garenoxacin, and moxifloxacin) in J774 macrophages. Antimicrob. Agents Chemother. *49*, 2429–2437. https://doi.org/10.1128/AAC.49.6.2429-2437.2005.

35. Turnidge, J. (1999). Pharmacokinetics and Pharmacodynamics of Fluoroquinolones. Drugs *58*, 29–36. https://doi.org/10.2165/00003495-199958002-00006.

36. Velkov, T., Bergen, P.J., Lora-Tamayo, J., Landersdorfer, C.B., and Li, J. (2013). PK/PD models in antibacterial development. Curr. Opin. Microbiol. *16*, 573–579. https://doi.org/10.1016/j.mib.2013.06.010.

37. Chanput, W., Mes, J.J., and Wichers, H.J. (2014). THP-1 cell line: An in vitro cell model for immune modulation approach. Int. Immunopharmacol. *23*, 37–45. https://doi.org/10.1016/j.intimp.2014.08.002.

38. Strobel, M., Pförtner, H., Tuchscherr, L., Völker, U., Schmidt, F., Kramko, N., Schnittler, H.-J., Fraunholz, M.J., Löffler, B., Peters, G., and Niemann, S. (2016). Post-invasion events after infection with Staphylococcus aureus are strongly dependent on both the host cell type and the infecting S. aureus strain. Clin. Microbiol. Infection *22*, 799–809. https://doi.org/10.1016/j.cmi.2016.06.020.

39. Grant, J., and Saux, N.L.; members of the Antimicrobial Stewardship and Resistance Committee ASRC of the Association of Medical Microbiology and Infectious Disease AMMI Canada (2021). Duration of antibiotic therapy for common infections. J. Assoc. Med. Microbiol. Infect. Dis. Can. *6*, 181–197. https://doi.org/10.3138/jammi-2021-04-29.

40. Nguyen, T.K., Peyrusson, F., Dodémont, M., Pham, N.H., Nguyen, H.A., Tulkens, P.M., and Van Bambeke, F. (2020). The Persister Character of Clinical Isolates of Staphylococcus aureus Contributes to Faster Evolution to Resistance and Higher Survival in THP-1 Monocytes: A Study With Moxifloxacin. Front. Microbiol. *11*, 587364. https://doi.org/10.3389/fmicb.2020.587364.

41. Ernst, E.J., Klepser, M.E., Petzold, C.R., and Doern, G.V. (2002). Evaluation of Survival and Pharmacodynamic Relationships for Five Fluoroquinolones in a Neutropenic Murine Model of Pneumococcal Lung Infection.

Pharmacotherapy *22*, 463–470. https://doi.org/10.1592/phco.22.7.463.33670.

42. Aranzana-Climent, V., Chauzy, A., and Grégoire, N. (2024). HF-App: A R-Shiny Application to Streamline Hollow-Fibre Experiments. R Application Version *1*. https://varacli.shinyapps.io/hollow_fiber_app/.

43. Tsuchiya, S., Yamabe, M., Yamaguchi, Y., Kobayashi, Y., Konno, T., and Tada, K. (1980). Establishment and characterization of a human acute monocytic leukemia cell line (THP-1). Int. J. Cancer *26*, 171–176. https://doi.org/10.1002/ijc.2910260208.

44. Peyrusson, F., Nguyen, T.K., Buyck, J.M., Lemaire, S., Wang, G., Seral, C., Tulkens, P.M., and Van Bambeke, F. (2021). In Vitro Models for the Study of the Intracellular Activity of AntibioticsMethods Mol. Biol.. In Bacterial Persistence, *2357*, N. Verstraeten and J. Michiels, eds. (Springer US), pp. 239–251. https://doi.org/10.1007/978-1-0716-1621-5_16

45. Prébonnaud, N., Chauzy, A., Grégoire, N., Dahyot-Fizelier, C., Adier, C., Marchand, S., and Aranzana-Climent, V. (2024). A freely accessible, adaptable hollow-fiber setup to reproduce first-order absorption: Illustration with linezolid cerebrospinal fluid pharmacokinetic data. Preprint at bioRxiv *22*, 463. https://doi.org/10.1101/2024.12.19.629487.

46. Seral, C., Van Bambeke, F., and Tulkens, P.M. (2003). Quantitative analysis of gentamicin, azithromycin, telithromycin, ciprofloxacin, moxifloxacin, and oritavancin (LY333328) activities against intracellular Staphylococcus aureus in mouse J774 macrophages. Antimicrob. Agents Chemother. *47*, 2283–2292. https://doi.org/10.1128/AAC.47.7.2283-2292.2003.

47. Lemaire, S., Kosowska-Shick, K., Appelbaum, P.C., Glupczynski, Y., Van Bambeke, F., and Tulkens, P.M. (2011). Activity of moxifloxacin against intracellular community-acquired methicillin-resistant Staphylococcus aureus: Comparison with clindamycin, linezolid and co-trimoxazole and attempt at defining an intracellular susceptibility breakpoint. J. Antimicrob. Chemother. *66*, 596–607. https://doi.org/10.1093/jac/dkq478.

STAR★METHODS

KEY RESOURCES TABLE

REAGENT or RESOURCE	SOURCE	IDENTIFIER
Bacterial and virus strains		
Staphylococcus aureus	ATCC	ATCC29213
Chemicals, peptides, and recombinant proteins		
Moxifloxacin-HCl	Bayer	CAS number: 186826-86-8
Ciprofloxacin-HCl	Bayer	CAS number: 86393-32-0
[^{2}H$_8$]-Ciprofloxacin	Alsachim	CAS number: 1130050-35-9
Gentamicin sulfate	PanReas AppliChem	Cat# A1492
RPMI 1640	Gibco	Cat# 21875091
Fetal bovine serum	Gibco	Cat# A5256701
Ca-MHB	Sigma-Aldrich	Cat# 90922
MHA	Sigma-Aldrich	Cat# 70191
Formic acid	Merck	Cat# 543804
Acetonitrile	J.T. Baker	Cat# JT9829
Charcoal	Merck	Cat# 05105
Critical commercial assays		
DC (detergent compatible) Protein Assay Kit II	Biorad	Cat# 5000112
Trypan blue	Gibco	Cat# 15250061
Experimental models: Cell lines		
THP-1 cells	ATCC	ATCC-TIB-202
Software and algorithms		
HF-app	Aranzana-Climent et al.[42]	https://varacli.shinyapps.io/hollow_fiber_app/
GraphPad Prism	Graphpad software	Version 8.0 www.graphpad.comm
Other		
Hollow fiber Helixone® cartridges	Fresenius Medical Care	Cat# 5008221
Neocap® obturator	Asept InMed	Cat# 202111
GL14 PP (polypropylene) screw caps	VWR	Cat# SCOT1156292
0.22 μM membrane filter	VWR	Cat# 554-3009
RythmicTM Perf + computerized perfusion pump	Micrel Medical Devices	Cat# KP5.04.274.2
high-flow Masterflex™ L/S™ peristaltic pump	VWR	Cat# 07522-30 (body) Cat# 77200-50 (head)
Plastipak syringe	BD Becton	Cat# 303175 (1mL) Cat# 300629 (20mL) Cat# 309653 (50mL)
NX-C18 LC column	Phenomenex	Cat# 00F-4454-B0

EXPERIMENTAL MODEL AND STUDY PARTICIPANT DETAILS

Drugs and chemicals

Moxifloxacin-HCl (MXF) and ciprofloxacin-HCl (CIP) were provided as microbiological standards by Bayer AG (Leverkusen, Germany); gentamicin sulfate was purchased from Medix Biochemica (St-Louis, MO); Roswell Park Memorial Institute (RPMI) 1640 medium and fetal bovine serum (FBS) were purchased from Gibco (Thermo Fisher Scientific, Waltham, MA); cation-adjusted Mueller-Hinton broth (CA-MHB) and Mueller-Hinton agar (MHA) were obtained from Sigma-Aldrich (St-Louis, MO).

Bacterial strain and cells

Staphylococcus aureus ATCC 29213 reference strain was acquired from the American Type Culture Collection (Manassas, VA) and freshly cultured before each experiment at 37°C in CA-MHB with shaking at 130 rpm. MICs were determined by microdilution in CA-MHB at physiological pH according to the guidelines of the Clinical and Laboratory Standards Institute (CLSI). THP-1 cells, a human

myelomonocytic cell line derived from the blood of a 1-year old boy that displays macrophage-like activity,[43] were maintained in our laboratory as previously described and freshly cultured before each experiment in RPMI 1640 supplemented with 10% Fetal Bovine Serum (FBS) at 37°C in a 5% CO_2 atmosphere.[44] The model being set-up for non-adhering cells, they were not further differentiated in macrophages.

METHOD DETAILS

Intracellular infection

Intracellular infection was conducted as previously described[30,31,44] with specific adaptations required for the performance of the experiments in the hollow fiber system (see results for justification of these changes). Briefly, the cells (5×10^5 cells mL^{-1}) were maintained as a loose suspension in RPMI 1640 medium supplemented with 10% FBS at 37°C under a 5% CO_2 atmosphere. The day before the infection, *S. aureus* culture was freshly prepared in 10 mL of CA-MHB (37°C, 130 rpm agitation) to reach a stationary-phase culture. The day of the experiment, bacteria were diluted at a ratio of 1:50 in fresh CA-MHB for 1h30 to ensure that the population was in log-phase growth. Bacteria were then opsonized during 45 min (37°C, 130 rpm) using non-decomplemented human serum diluted 1:10 in serum-free culture medium (RPMI 1640). Phagocytosis was subsequently allowed at a low bacterium-macrophage ratio (MOI, multiplicity of infection) of 0.0001:1 for 45 min. Elimination of the non-phagocyted bacteria was achieved by incubation during 1 h with gentamicin (25 μg mL^{-1}; 50 x MIC), followed by three washing steps with phosphate-buffered saline (PBS) and centrifugation at 1,300 rpm for 7 min. Infected cells were then resuspended in prewarmed complete RPMI (10% FBS) during 12 h in order to reach an average infection index (MOI) of 4 bacteria per macrophage (MOI = 4:1) (as determined by counting the numbers of colonies forming units (CFU)). This protocol resulted in a final intracellular inoculum of approximately 10^6 CFU mg cell protein^{-1}.

Hollow fiber infection model (HFIM)

The HFIM was used to assess bacterial responses to clinically relevant PK profiles. This system is composed of a dialysis cartridge linked to a central reservoir, which is further connected to two additional compartments: a waste reservoir and a diluent reservoir (see[14,45] for an overall review of this system). Fluid movement between compartments is facilitated by tubing and controlled via peristaltic pumps. Antibiotic is administered through an additional pump connected to the central reservoir (see Figure S1 for system configuration). The set-up of the model is detailed in the next paragraphs. The results were subsequently compared with those obtained from traditional TKC experiments.[10,46]

Materials

All experiments were conducted using RPMI 1640 medium supplemented with a reduced concentration of 2% FBS.[15] The hollow fiber system was incubated at a temperature of 37°C under a 5% CO_2 atmosphere. Hollow fiber Helixone cartridges were procured from Fresenius Medical Care (FX-PAED Helixone dialyzer, Bad Homburg, Germany), with a Neocap obturator (Asept InMed, Quint-Fonsegrives, France) placed on the top of the cartridge to facilitate the collection of samples for pharmacokinetic and pharmacodynamic (PK/PD) analysis within the cartridge. The extracapillary space (ECS) of each cartridge has a 60 mL capacity. The central reservoir was constituted of a 500 mL bottle, pre-filled with 300 mL RPMI 1640 with 2% FBS. It was equipped with a connection system featuring two PTFE (polytetrafluoroethylene) ports secured with GL14 PP (polypropylene) screw caps (VWR, Radnor, Pennsylvania, US), equipped with a 0.22 μM membrane filter to facilitate pressure equalization (VWR) and was continuously mixed using a magnetic stirrer.

The diluent medium, composed of RPMI complete medium (2% FBS), was prepared in a 5 L borosilicate glass bottle (VWR), closed using a connection system incorporating two PTFE ports with GL14 PP screw caps and also equipped with a 0.22 μM membrane filter to facilitate pressure equalization (VWR). The diluent medium was extended to the bottom of the media bottle using platinum-cured silicone tubing and secured with a GL14 screw cap insert. The medium was subsequently pumped into the central reservoir using a peristaltic pump. To maintain a constant volume within the system, the addition of fresh medium to the central reservoir was balanced by the simultaneous removal of an equivalent volume to the waste reservoir. Antibiotics were added in the central reservoir via a Rythmic Perf + computerized perfusion pump (Micrel Medical Devices, Koropi, Attiki, Greece). A second obturator was positioned on a three-way stopcock between the central reservoir and the cartridge to enable sample collection for PK measurement in the central compartment. Rapid equilibration of antibiotic concentration between the central compartment and the cartridge was ensured through a high-flow Masterflex L/S peristaltic pump (VWR) operating at a rate of 60 mL min^{-1}. Prior to the assembly of the system, the medium was filtered through a 0.20 μM pore size vacuum filtration apparatus (VWR).

THP-1 human monocytes were concentrated to a density of 5×10^5 cells mL^{-1} and infected with *S. aureus* as described above before being inoculated into the 60 mL dialysis cartridge via a BD Plastipak syringe (50 mL BD Becton; Dickinson and Company, Franklin Lakes, New Jersey, US).

Set-up

The hollow fiber system, free from bacteria or cells, was set up and incubated at 37°C before the start of the experiment. Twelve hours before the addition of antibiotic (time point T0), *S. aureus* infected THP-1 cells were introduced into the cartridge, which was subsequently

positioned within the system and incubated without renewal of the medium. Preliminary experiments showed that this step was critical for facilitating: 1) the proliferation of the initial inoculum to reach a high enough concentration to allow further bacteria growth but low enough to avoid killing the host cells (typically 10^6 CFU mg cell protein^{-1}), and 2) the adaptation of the infected cells to this new environment. After this preincubation period, the system was activated for 1 h at 60 mL min^{-1} to enable medium renewal within the cartridge. An initial sample was taken to determine the initial inoculum at this time point, defined as (T0) for experiments where the antibiotic was added at that time. Each antibiotic was administered as a 5 mL 1-h infusion, with ciprofloxacin dosed once every 12-h at a concentration of 242.91 μg mL^{-1} and moxifloxacin dosed once every 24-h at a concentration of 179.95 μg mL^{-1}. Diluent medium was subsequently pumped into the central reservoir using a peristaltic pump at a flow rate of 2.31 mL min^{-1} for ciprofloxacin and 0.49 mL min^{-1} for moxifloxacin, to mimic the pharmacokinetic (PK) profiles of the antibiotics. Experiments were conducted over 36 h for each antibiotic tested, consisting of 12 h of incubation, an additional 1 h for medium renewal within the cartridge, and 24 h for sampling to evaluate the activity of the antibiotics.

Simulation of PK profiles in the HFIM

In this study, we simulated the PK profiles of ciprofloxacin and moxifloxacin administered via the intravenous route (IV) at doses of 400 mg twice daily and 400 mg once daily, respectively. Key parameters such as maximum serum concentration (Cmax), infusion time (Tinf), dosing interval (τ), half-lives (T1/2) were obtained from the study of Lettieri et al.[20] for ciprofloxacin and of Stass et al.[21] for moxifloxacin (see Table 1). Both studies evaluated total plasma concentrations. As the serum concentrations in culture media were low (2%), the protein concentrations were low thus these values were adjusted to mimic protein-unbound pharmacokinetic profiles. A protein-bound fraction in plasma of 30% for ciprofloxacin[20] and 40% for moxifloxacin[21] were considered. The simulations of target profiles were conducted using the HF-app, a web application developed with R-shiny by Vincent Aranzana-Climent et al. (INSERM U1070, Poitiers, France).[42] This tool was designed to streamline the calculations involved in setting up hollow-fiber experiments for both single-drug and combination therapies.

Pharmacokinetic (PK) measurements in HFIM

Sampling was performed as follows: the central compartment of the HF system was sampled (500 μL) just before the addition of the antibiotic (T0) and at multiple time points post-administration of the antibiotic in order to validate its concentration-time profile. In parallel, the cartridge was sampled (1 mL) to measure the antibiotic concentrations directly in contact with bacteria, to take into account the penetration of the antibiotic in the extracapillary space within the cartridge. This sample was also used for PD determination (see PD measurement section). For antibiotic intracellular concentrations, after cell lysis for PD measurements (see TKC protocol), an aliquot of 50 μL was taken for analysis. (see Figure S1 supplementary material).

Both drugs ware assayed by HPLC-MS/MS

To establish calibration standards, stock solutions of antibiotics were prepared at 0.1 mg mL^{-1} in distilled water. Working solutions for calibration curves were prepared at concentrations ranging from 5000 to 5 ng mL^{-1} for ciprofloxacin and from 2000 to 5 ng mL^{-1} for moxifloxacin. These dilutions were performed in water with formic acid 0.1% for the intracellular calibration curve and in RPMI +10% FBS for the extracellular calibration curve. The working solutions corresponding to the intracellular calibration curve were individually spiked with dry THP-1 cell pellets at a density of approximately 2×10^6 cells per pellet. Subsequently, aliquots of each sample and each solution from the calibration curves (50 μL) were transferred into a 1.5 mL centrifuge tube and mixed with 25 μL of IS ([^{2}H$_8$]-Ciprofloxacin at a concentration of 0.4 μg mL^{-1} in distilled water for ciprofloxacin, and ciprofloxacin at a concentration of 0.8 μg mL^{-1} in distilled water for moxifloxacin). Deproteinization was then achieved by the addition of 200 μL of acetonitrile with 0.1% formic acid followed by vortexing for 5 s. All samples were further centrifuged at 14,000 rpm at 4°C for 10 min. Lastly, 180 μL of the supernatants were transferred to an HPLC vial containing 20 μL of water with formic acid 0.2% for analysis. For moxifloxacin, the extracted samples were diluted 3 times in acetonitrile with formic acid 0.1% to ensure being in the linear range of the calibration curve. Samples were stored at 4°C until analysis.

Samples were analyzed by the Triple Quad LC-MS method (Shimadzu Corporation, Kyoto, Japan). Both ciprofloxacin and moxifloxacin separation were achieved at ambient temperature on a 150 mm × 2 mm, 5 μM Gemini NX-C18 LC column (Phenomenex, Torrance, CA, US). The mobile phase consisted of water with 0.1% formic acid and acetonitrile with 0.1% formic acid in a ratio of 75:25, which was pumped into the chromatographic system under isocratic conditions at a flow rate of 0.2 mL min^{-1}. The injection volume of the sample was 20 μL, and the samples were maintained in a thermostatic autosampler (4°C). The total analysis time was 7.5 min, with elution of ciprofloxacin and [^{2}H$_8$]-ciprofloxacin occurring at 1.93 min and moxifloxacin at 1.92 min. The transitions from precursor to product ions for CIP were 331.4 m/z to 314 m/z, 339.2 m/z to 321.1 m/z for [^{2}H$_8$]-Ciprofloxacin, and 402.1 m/z to 384.1 m/z for moxifloxacin. The quantifiable ranges established by the methods were from 5 to 0.005 μg mL^{-1} for ciprofloxacin and from 2 to 0.005 μg mL^{-1} for moxifloxacin. The peak area ratios of ciprofloxacin and moxifloxacin relative to their respective IS across each standard solution were calculated and subsequently plotted as a function of drug concentrations. The calibration curves were acceptable only when exhibiting correlation coefficients (r^2) equal to or exceeding 0.98. Data acquisition was processed using Shimadzu LabSolutions software version 5.109.

Pharmacodynamic (PD) measurements in HFIM

For each sample, the bacterial load was assessed extracellularly and intracellularly. The content of the cartridge was vigorously mixed using two 20-mL syringes (BD Becton), from which a 1 mL suspension was extracted through an obturator. These samples were then processed as described for TKC experiments.

Time kill-curves (TKC)

The experiments were conducted concurrently with HFIM to evaluate the effects of antibiotics under static conditions (TKC) in comparison to dynamic conditions. TKC were performed as described earlier with some modifications.[10,46] Cells infected as described above were plated into 12-well plates (2 mL per well) and incubated for 12 h (37°C, 5% CO_2 atmosphere) to achieve a MOI of 4:1, *i.e.*, a value corresponding to that obtained using the originally described model of intracellular infection.[10,30,31] At that time, the antibiotic was added at its maximal unbound concentration in human serum (Cmax; 2.8 µg mL^{-1} for ciprofloxacin and 2.4 µg mL^{-1} for moxifloxacin for an administered dose of 400 mg)[20,21] in each well or at concentrations allowing to mimic the unbound area under the curve (AUC) in human serum over 24 h, corresponding to 1.1 µg mL^{-1} for moxifloxacin (equivalent to an AUC_{24h} of 26.41 mg h L^{-1})[21] and 0.7 µg mL^{-1} for ciprofloxacin (equivalent to an AUC_{12h} of 17.31 mg h L^{-1}).[20] Samples of 1 mL were collected at various time points: 0 h (before the addition of the antibiotic) and 0.5, 1, 2, 4, 6, 8, 10, 12, 22, and 24 h after the addition of the antibiotic (1 well per time point). After centrifugation at 1,300 rpm for 7 min, 100 µL of the supernatant was spread on MHA + charcoal (2%) agar plates (20 mL) after appropriate dilutions in PBS for quantification of extracellular CFU counts. Charcoal addition aimed at adsorbing residual antibiotic and avoiding carry-over effect.[47] The extracellular bacteria detected at this stage reflect the bacterial inoculum released due to the natural death of infected THP-1 cells during the incubation period. The remaining supernatant was then carefully removed, and the pellet resuspended in 1 mL of PBS and centrifuged again at 1,300 rpm for 7 min to eliminate any remaining extracellular bacteria. PBS was removed, and the pellet was resuspended in 500 µL of distilled water for 5 min to lyse the cells. A 100 µL aliquot of lysate was plated on MHA + charcoal (2%) agar plates (20 mL) after appropriate dilutions in PBS for quantification of the number of viable intracellular bacteria through colony counting. Forty µL were also used for total cell protein measurement using a DC (detergent compatible) Protein Assay from Bio-Rad (Hercules, CA) according to the manufacturer's instructions. Data were expressed as the number of CFUs per milligram of cell protein (CFUs mg cell protein^{-1}) for intracellular bacteria and as the number of CFUs per milliliter (CFUs mL^{-1}) for extracellular bacteria.

Cell viability

Cell viability was evaluated in wells (TKC) and HFIM for non-infected and infected cells using the Trypan blue exclusion assay according to the provider's instructions (Gibco, Thermo Fisher Scientific). After harvesting and washing the cells in PBS, they were stained at a 1:1 ratio with Tryptan blue solution 0.4%. After mixing, 10 µL of the suspension was pipetted into a Burker counting chamber, and cells were counted according to the manufacturer's instructions. The percentage of mortality was expressed as the ratio between the number of blue-stained cells (dead) and the total number of cells in a specified surface area.

QUANTIFICATION AND STATISTICAL ANALYSIS

Experiments to set up de model were performed in triplicates in a single experiment; but viability and MOI were checked again in all further experiments. Experiments to determine pharmacokinetic profiles and activity were performed in 2 or 3 independent replicates. Plotting and calculations were performed using GraphPad Prism version 8.0 (GraphPad software, San Diego, CA). Observed PK parameters were determined using exponential decay model on GraphPad. Statistical analyses were performed to assess treatment efficacy, THP-1 viability, and to determine the right MOI, using 95% confidence intervals (CI) to assess the precision of our measurements. For each treatment group, CI were calculated using GraphPad to quantify the uncertainty around each mean estimate. These intervals were interpreted to determine both the reliability of the observed effects and the statistically significant effect between groups. When comparing group means, a non-overlapping CI was considered indicative of a statistically significant difference between treatment effects. For other comparisons between two groups, student t-tests for independent samples were performed (differences were considered as significant if *p* values were <0.05 [*p* < 0.05]). All details about the number of replicates and the way data are represented (with SD, SEM or confidence interval) are indicated in the captions of the figures or footnotes to tables.